One-shot Underwater Active Stereo Through Refractive Parallel Flat Surfaces

Meng-Yu Jennifer KUO† and Shohei NOBUHARA††

† Graduate School of Informatics, Kyoto University　Yoshida Honmachi, Sakyo, Kyoto, 606-8501
E-mail: †jennifer@vision.kuee.kyoto-u.ac.jp, ††nob@i.kyoto-u.ac.jp

Abstract　This paper presents a novel one-shot underwater active stereo system that realizes a dense 3D shape reconstruction of underwater objects. Real-time active scanning in underwater environment has been a difficult task due to the encountered challenges associated with refraction, scattering, absorption, etc. In the case with refraction, image-based correspondence search using epipolar geometry is invalid. The main contribution of this paper is the development of a practical algorithm to estimate the projector pixel locations from an observed image with a projected grid pattern in underwater environment. More precisely, the one-to-one correspondence between the projector and camera pixels was successfully established by employing the co-planarity constraint between 3D rays in water emitted from the camera and the projector.

Key words　Underwater Active Stereo, One-shot Structured Light Systems, Refraction

1. Introduction

3D analysis of underwater objects can be widely used in various applications. For instances, monitoring the development process of fertilized eggs can be contributed for bioinformatics; underwater projection mapping can be employed as an educational interactive system in the aquarium, etc. However, 3D scanning in underwater environment has been a difficult task due to the encountered challenges associated with refraction, scattering, absorption, etc., which indicates that we cannot simply apply the conventional vision techniques for the geometric modeling.

One of the main techniques for 3D shape reconstruction is done by using the corresponding locations among different views. Compared to the passive stereo techniques, the correspondence search becomes much easier in active stereo system which basically consists of a camera and a projector due to the uniqueness and distinctiveness of the features in the projected patterns. In general, we project multiple regular structured light patterns such as Gray-coded patterns, phase shifting Gray-coded patterns, etc. onto the objects to estimate the one-to-one correspondence between camera and projector. In order to realize the active scanning in the dynamic environment, one-shot active stereo system has become one of the main techniques [6]〜[9], which remarkably improves the efficiency of correspondence search.

In contrast to regular structured light patterns, the correspondence search through one-shot pattern techniques in the air environment can be solved efficiently by epipolar geometry due to the co-planarity among the 3D point of the object and its corresponding 2D points on camera/projector image planes (Fig. 1). However, since the camera and projector are usually arranged in a specific housing in the underwater environment, the refraction phenomenon encountered in this housing needs to be addressed into the process of correspondence estimation. More precisely, in the case with refraction, such correspondence search process is strongly disturbed because of the depth-dependent refractive distortions, which indicates that the co-planarity which is given by epipolar geometry is no longer available (Fig. 2). Thus, it is necessary to look for an efficient way to enable this epipolar assumption.

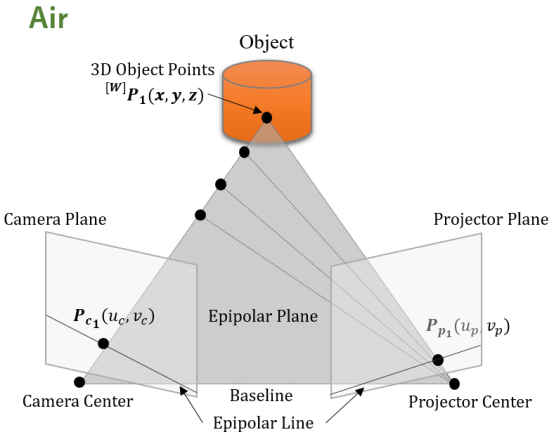

Fig. 1　Epipolar geometry without refraction

The objective of this study is to establish a novel one-shot underwater active stereo system that realizes the dense 3D shape reconstruction of underwater objects.

2. Related Works

Studies related to calibration models for underwater camera have been developed for many years [2]〜[6], [10], while none of them provides a practical strategy for calibration and re-

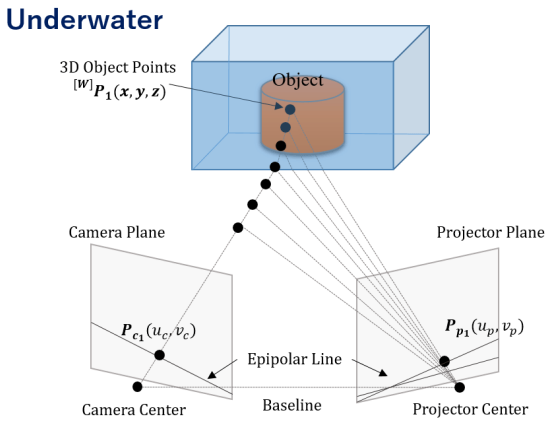

Fig. 2 Epipolar geometry with refraction

construction procedures in the structured light systems(SLS). Besides, some of the proposed models even become invalid due to the problems that occur during the process of correspondence search in SLS.

In order to handle the refraction problem through parallel flat surfaces, Agrawal et al. have proposed a unified calibration technique with multiple layers since the geometry of rays in such system corresponds to an axial camera model [1]. In their work, they derive forward and backward projection equations for their refractive model. However, it requires solving a 4th degree equation even if there is only one refractive plane, and requires solving a 12th degree equation in the two refractive planes cases for the forward (3D-to-2D) projection, which may be a time-consuming process. Kawahara et al. proposed pixel-wise varifocal camera model(PVCM) with an efficient underwater forward (3D-to-2D) projection technique through two parallel flat surfaces as well as a calibration method for underwater projector-camera system [4]. They modeled a non-central projection of the underwater cameras where the focal lengths of the projection are varied pixel-by-pixel. They also proposed an underwater active-stereo system consisted of two cameras and one projector that captures the 3D information of dynamic objects in water such as swimming fish based on their model. As image-based correspondence searching using epipolar geometry is invalid in underwater environment, they applied space carving method for the reconstruction procedure instead.

In terms of one-shot SLS for 3D shape reconstruction of fast moving objects, a region-wise method that projects only a single grid pattern consisting of sets of parallel color-coded lines in the air environment has been proposed [7]. Compared to the regular structured light patterns, this grid pattern cannot tell the absolute corresponding points in the projector image directly on a pixel basis since the one-shot projection encodes the pixel position up to two unknown shifts. Instead, the proposed method detects continuous regions in the camera image sharing such unknowns in order to resolve the ambiguity by a per-region manner.

In the study of underwater active one-shot 3D scanning, the depth-dependent refractive distortions have been modeled through a polynomial approximation method [6]. In this method, it depth-dependently calibrates the parameters associated with the active scanning system with the projection of a static wave pattern. However, this approximation method will inevitably cause some errors on the epipolar lines which indicates that the accuracy of the reconstruction result will definitely be influenced. Besides, the depth-dependent calibration parameters will also cause the inconsistency of the reconstructed shape due to the sparse set of depth values.

In our study, we only considered the refraction occurred in underwater environment, and assumed that the rest of the complex light phenomenon can all be ignored. We would employ a virtual camera model to handle the depth-dependent refractive distortion encountered in the refractive medium geometrically, and deal with the problem of image correspondence matching through the employment of refractive epipolar geometry with a one-shot pattern. The accuracy of the 3D capturing of underwater objects would also be evaluated.

3. Calibration

3.1 Measurement Model and Its Calibration

3.1.1 Single Underwater Camera

A single underwater camera model can be illustrated in Fig. 3. Since the housing contains two flat surfaces that are parallel to each other, we employed a virtual axial camera model [1], which is placed at the same location as the real underwater camera and its optical axis is in the same direction along the normal vector $\mathbf{n}$ of the refractive parallel flat surfaces, to simplify the pinhole model without loss of generality (Fig. 4).

Based on the underlying geometry of the rays, the refractive indices and layer thicknesses can be computed easily. As shown in Fig. 4, the light path $l_c^a - l_c^g - l_c^w$ is derived from the observed points $p_c^{[AC]}(i)$ and passed through the intersection points $p_c^a(i), p_c^g(i)$ on housing. Denote $\vec{v}_c^x$ as the direction vectors of l_c^x toward water from the camera center, where $x \in \{a, g, w\}$ represents each media. Denote μ_a, μ_g, μ_w as the refractive indices of each media, and τ_a^c, τ_g^c as the thicknesses between camera center and the first layer of the housing, and the thickness of the housing itself. The Snell's law can be expressed as

$$\mu_a \sqrt{x^2_{\vec{v}_p^a} + y^2_{\vec{v}_p^a}} = \mu_g \sqrt{x^2_{\vec{v}_p^g} + y^2_{\vec{v}_p^g}} = \mu_w \sqrt{x^2_{\vec{v}_p^w} + y^2_{\vec{v}_p^w}}. \quad (1)$$

Let $r_c = \sqrt{x^2_{p_c^{[AC]}} + y^2_{p_c^{[AC]}} + z^2_{p_c^{[AC]}}}$. Then the direction vectors $\vec{V}_c^x$ and the intersection points p_c^a, p_c^g can be obtained as follows,

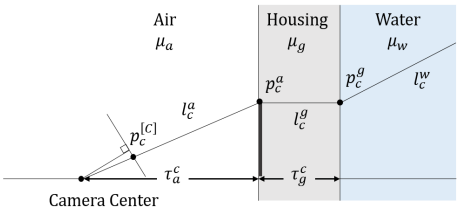

Fig. 3 Pinhole camera model

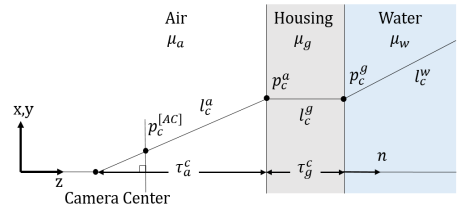

Fig. 4 Axial camera model

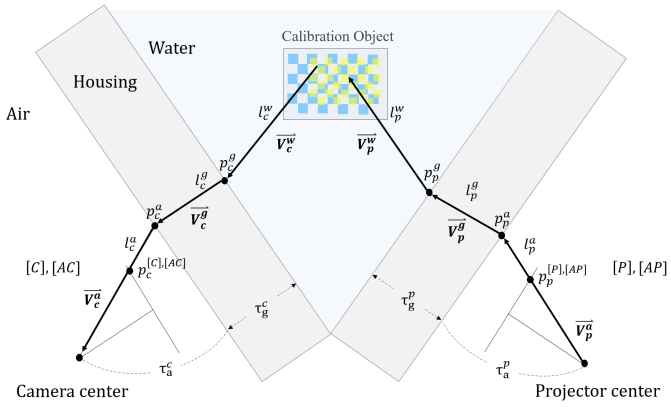

Fig. 5 Measurement model of underwater projector-camera system

$$
\begin{aligned}
\vec{V}_c^a &= \left(\frac{x_{p_c^{[AC]}}}{r_c}, \frac{y_{p_c^{[AC]}}}{r_c}, \frac{z_{p_c^{[AC]}}}{r_c}\right),\\
p_c^a &= \frac{\vec{V}_c^a}{z_{\vec{v}_c^a}}\tau_a^c,\\
\vec{V}_c^g &= \left(\frac{\mu_a}{\mu_g}x_{\vec{v}_c^a}, \frac{\mu_a}{\mu_g}y_{\vec{v}_c^a}, \sqrt{1-(x_{\vec{v}_c^g}^2+y_{\vec{v}_c^g}^2)}\right),\\
p_c^g &= p_c^a + \frac{\vec{V}_c^g}{z_{\vec{v}_c^g}}\tau_g^c,\\
\vec{V}_c^w &= \left(\frac{\mu_g}{\mu_w}\sqrt{x_{\vec{v}_c^g}^2+y_{\vec{v}_c^g}^2}\frac{x_{\vec{v}_c^a}}{\sqrt{x_{\vec{v}_c^a}^2+y_{\vec{v}_c^a}^2}},\right.\\
&\left.\frac{\mu_g}{\mu_w}\sqrt{x_{\vec{v}_c^g}^2+y_{\vec{v}_c^g}^2}\frac{y_{\vec{v}_c^a}}{\sqrt{x_{\vec{v}_c^a}^2+y_{\vec{v}_c^a}^2}}, \sqrt{1-(x_{\vec{v}_c^w}^2+y_{\vec{v}_c^w}^2)}\right).
\end{aligned}
\tag{2}
$$

3.1.2 Underwater Projector and Camera

As shown in Fig. 5, the camera and projector are arranged in a specific housing. The planar plane in water is used for the calibration process. Due to the reversibility of the light, the underwater projector can be viewed as a reversed underwater camera and hence we can model the rays emitted from the projector in the same way as described in previous section.

3.2 Calibration of Single Underwater Camera

The calibration of our single underwater camera model can be done based on the method described in [1], which estimate the parameters of refraction.

We first attach a chessboard pattern on housing in the water side. The 2D points of the chess corners $p_c^{[C]}$ can be detected in a captured camera image. Here we assume the intrinsic camera calibration has been done beforehand and thus we know the camera ray $v(i)$ for each 3D point of the chess corners $q_g(i)$. Denote R_v as the rotation matrix between the virtual axial camera model and pinhole camera model, and T_v as the translation matrix between the virtual axial camera model and the chessboard pattern. The transformed 3D point $q_g + T_v$, the corresponding transformed camera ray $R_v p_c^{[C]}$, and the normal vector n are all lied on the same plane. Thus, the coplanarity constraint between the 3D points on the chessboard and the virtual axial camera rays can be shown as follows,

$$
(q_g + T_v)\cdot\left((0,0,1)^T \times R_v p_c^{[C]}\right) = \vec{0}. \tag{3}
$$

By rewriting the above equation, we then have

$$
\begin{pmatrix}
x_{p_c^{[C]}}y_{q_g}\\
x_{p_c^{[C]}}\\
-x_{p_c^{[C]}}x_{q_g}\\
y_{p_c^{[C]}}y_{q_g}\\
y_{p_c^{[C]}}\\
-y_{p_c^{[C]}}x_{q_g}\\
z_{p_c^{[C]}}y_{q_g}\\
z_{p_c^{[C]}}\\
-z_{p_c^{[C]}}x_{q_g}
\end{pmatrix}^T
\begin{pmatrix}
r_{11}\\
r_{11}t_2 - r_{21}t_1\\
r_{21}\\
r_{12}\\
r_{12}t_2 - r_{22}t_1\\
r_{22}\\
r_{13}\\
r_{13}t_2 - r_{23}t_1\\
r_{23}
\end{pmatrix} = \vec{0}. \tag{4}
$$

If i points are observed in the captured camera image, by stacking i such equations we can obtain in matrix form as $Ax = 0$, where A is a $n \times 9$ matrix. if $i \geq 9$, we will have in general a unique solution x defined up to a scale factor. The solution to Eq (4) is well known as the eigenvector of A^TA associated with the smallest eigenvalue.

Denote $p_g(x_{p_g}, y_{p_g}, z_{p_g})$ as the intersection point on second layer of housing. By using Snell's law, we can describe point p_g as follows,

$$
\begin{aligned}
\sqrt{x_{p_g}^2+y_{p_g}^2} &= \frac{\sqrt{x_{\vec{v}_p^a}^2+y_{\vec{v}_p^a}^2}}{z_{\vec{v}_p^a}}\tau_a^c + \frac{\sqrt{x_{\vec{v}_p^g}^2+y_{\vec{v}_p^g}^2}}{z_{\vec{v}_p^g}}\tau_g^c\\
&= \frac{\sqrt{x_{\vec{v}_p^a}^2+y_{\vec{v}_p^a}^2}}{z_{\vec{v}_p^a}}\tau_a^c + \frac{\mu_a}{\mu_g}\frac{\sqrt{x_{\vec{v}_p^a}^2+y_{\vec{v}_p^a}^2}}{\sqrt{1-\frac{\mu_a^2}{\mu_g^2}(x_{\vec{v}_p^a}^2+y_{\vec{v}_p^a}^2)}}\tau_g^c,
\end{aligned}
\tag{5}
$$

where τ_a^c, τ_g^c and μ_a, μ_g are the thicknesses and the refractive indices of each media. Assume $\mu_a = 1$ and set $r_{p_g} =$

$\sqrt{x_{p_g}^2 + y_{p_g}^2}$, $r_{\vec{v}_p^a} = \sqrt{x_{\vec{v}_p^a}^2 + y_{\vec{v}_p^a}^2}$, and $\tan\theta_a = \frac{r_{\vec{v}_p^a}}{z_{\vec{v}_p^a}}$. Eq (5) then can be rewritten as

$$\begin{pmatrix} r_{p_g}^2 \\ -\tan\theta_a^2 \\ \tan\theta_a^2 r_{\vec{v}_p^a}^2 \\ -r_{\vec{v}_p^a}^2 \end{pmatrix}^T \begin{pmatrix} \mu_g^2 \\ \mu_g^2 \tau_a^{c^2} \\ \tau_a^{c^2} \\ \tau_g^{c^2} \end{pmatrix} = r_{p_g}^2 r_{\vec{v}_p^a}^2. \qquad (6)$$

Given m points in the captured image, we can stack all equations together to obtain in matrix form as $Ax = b$, where $x = [\mu_g^2, \mu_g^2\tau_a^{c^2}, \tau_a^{c^2}, \tau_g^{c^2}]^T$. Then the linear least-square solution is given by

$$x = (A^T A)^{-1} A^T b. \qquad (7)$$

Finally, we refine all of the parameters $R_v, T_v, \tau_a^c, \tau_g^c, \mu_g$ by a re-projection error minimization.

3.3 Calibration of Underwater Projector-Camera System

The goal of this part is to estimate the relative pose of the projector and the camera from images with refractive distortions. The projector can be calibrated by providing the 3D positions of the projected chess corners in water by the camera that calibrated before (Fig. 5) as described in [4]. In practice, the overall process can be described as follows,

1 Estimate the relative pose R_c, T_c between the virtual axial camera and the planar chessboard pattern placed in water.

2 Project the other chessboard pattern on the model plane by projector and estimate its 3D positions using the calibrated camera parameters.

3 Estimate the relative pose R_p, T_p between the underwater projector and the model plane by using 2D-to-3D correspondences of the projected chess corners.

4 Compute the thicknesses τ_a^p, τ_g^p of each media based on the principle of Snell's law.

5 Derive the relative pose R_p', T_p' between the virtual axial projector and the model plane.

6 Estimate the relative pose R_{p2c}, T_{p2c} between the virtual projector and the virtual camera by using the pre-calibrated parameters.

7 Refine all parameters by minimizing the re-projection error.

4. One-shot Correspondence Search of Underwater Projector-Camera System

4.1 One-shot Pattern Decoding

In contrast to the regular structured light system, one-shot pattern yields a higher efficiency for the image-based correspondence search.

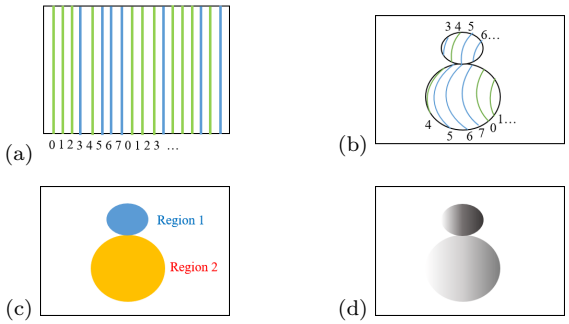

Fig. 6 An example of color-coded line pattern decoding: (a) projected pattern, (b)camera captured image with decoded ID, (c) region segmentation, (d) unwrapped image.

In our work, we employed a color-coded line pattern [7] which provides non-unique correspondences up to two degrees of freedom, one is for horizontal direction and the other one is for vertical direction.

More precisely, the lines are first decoded into IDs which are assigned from 0 to 7 based on the principle of de Bruijn sequence (Fig. 6(a) and Fig. 6(b)). The interpolation is then employed between each line for obtaining the values that are not on the lines. Because of the inevitable ambiguity occurs in the periodically encoded lines pattern, it cannot tell the exact corresponding projector pixel location. Instead we define the part that has continuous interpolated information as the same region (Fig. 6(c)), and then unwrap it in each region separately (Fig. 6(d)). A pair of shifting values is then added to each pixel in the same region for the estimation of exact corresponding coordinates of projector. In other words, each pixel in the same region has the corresponding coordinate of the projector with a pair of common unknown shifts $\text{shift}_x, \text{shift}_y$, which are used to adjust the relative position to the absolute one (Fig. 7).

In the case without refraction, this ambiguity can be solved easily by utilizing the co-planarity constraint which is given by epipolar geometry. However, in the case with refraction, this co-planarity constraint among the corresponding rays in the air becomes invalid.

4.2 Correspondence Search of Underwater Projector-Camera System

In order to realize underwater projector-camera correspondence search using the relative corresponding information obtained in the previous section, we employ the co-planarity constraint between 3D rays in water. As shown in Fig. 8, after transforming the two direction vector $\vec{V_c^w}, \vec{V_p^w}$ emitted from the camera and the projector, and the direction vector emitted from p_c^g to p_p^g in the water to the same coordinate

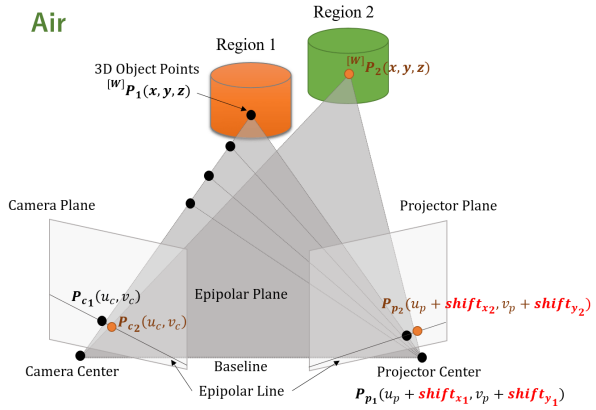

Fig. 7 Region-wise method using epipolar geometry in the air

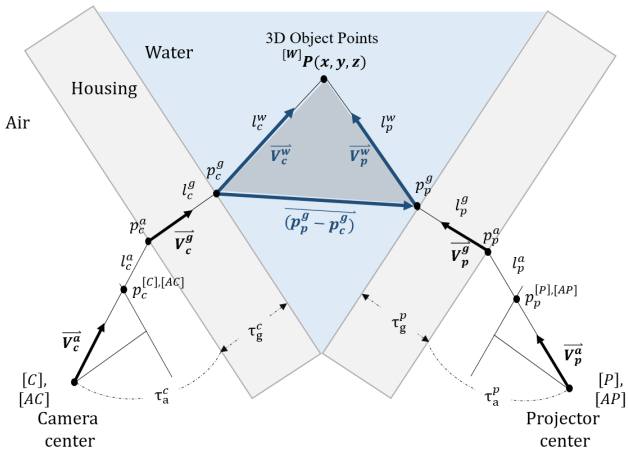

Fig. 8 Underwater co-planarity

system (e.g. underwater virtual axial camera model), these three vectors are lied on the same plane. Therefore, the co-planarity constraint between these three 3D rays in water can be shown as

$$\vec{V}_c^w \cdot \left((R_{p2c} p_p^g + T_{p2c} - p_c^g) \times (R_{p2c} \vec{V}_p^w) \right) = 0, \qquad (8)$$

where R_{p2c}, T_{p2c} are the transformation matrices from virtual axial projector to virtual axial camera. The unknown shifts $\text{shift}_x, \text{shift}_y$ are included in the intersection point p_p^g on the housing as well as its corresponding direction vectors $\vec{V}_p^w$ in Eq (8), which are derived from the corresponding point $p_p(u_p + \text{shift}_x, v_p + \text{shift}_y)$ in the projector image plane. Such unknown shifts $\text{shift}_x, \text{shift}_y$ can be estimated by solving Eq (8) with a nonlinear optimization method (e.g. Levenberg-Marquart algorithm).

5. Underwater 3D Shape Reconstruction

Up to this point, calibration parameters as well as the image-based correspondences of underwater projector-camera system required for 3D shape reconstruction have all been estimated.

The procedure of 3D shape reconstruction can be done by employing the linear triangulation. Here the 3D points $^{[W]}P(x_{[W]P}, y_{[W]P}, z_{[W]P})^T$ of the underwater object can be described as

$$\begin{aligned} x_{[W]P} &= \frac{x_{\vec{v}_{c,p}^w}}{z_{\vec{v}_{c,p}^w}} z_{[W]P} + x_{p_{c,p}^g}, \\ y_{[W]P} &= \frac{y_{\vec{v}_{c,p}^w}}{z_{\vec{v}_{c,p}^w}} z_{[W]P} + y_{p_{c,p}^g}. \end{aligned} \qquad (9)$$

After rewriting the above equation, we have

$$\begin{pmatrix} 1 & 0 & -\frac{x_{\vec{v}_{c,p}^w}}{z_{\vec{v}_{c,p}^w}} \\ 0 & 1 & -\frac{y_{\vec{v}_{c,p}^w}}{z_{\vec{v}_{c,p}^w}} \end{pmatrix} {}^{[W]}P(x_{[W]P}, y_{[W]P}, z_{[W]P})^T = \begin{pmatrix} x_{p_{c,p}^g} \\ y_{p_{c,p}^g} \end{pmatrix}. \qquad (10)$$

Given m pairs of corresponding points between the camera and the projector, we then can stack all equations together to obtain in matrix form as $M\,{}^{[W]}P = b$, where M is a $4m \times 3$ matrix. The linear least-square solution is given by

$${}^{[W]}P = (M^T M)^{-1} M^T b. \qquad (11)$$

6. Evaluation

6.1 Experimental Setup

The environmental setup can be shown in Fig. 9. In our system, we used one camera with 1280×960 resolution (Point-grey Flea3 FL3-U3-88S2C-C) and one 1080p projector(BenQ MH680) to realize the underwater active stereo system for 3D surface capturing. The projector-camera system was placed around an octagonal water tank of 900 mm diameter. The intrinsic calibrations of both camera and projector are done beforehand in the air and the relative pose between the camera and the projector was calibrated by the method described in Section 3. The captured object with the projected grid pattern was placed in the water tank and observed by the camera and the projector via two parallel flat tank surfaces where the thickness is about 30 mm. The light paths would go through air/glass and glass/water.

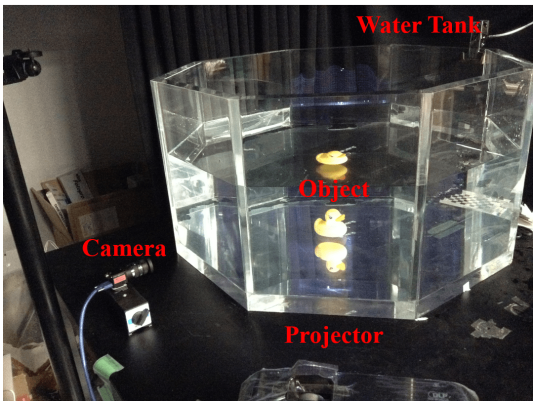

Fig. 9 Environmental setup

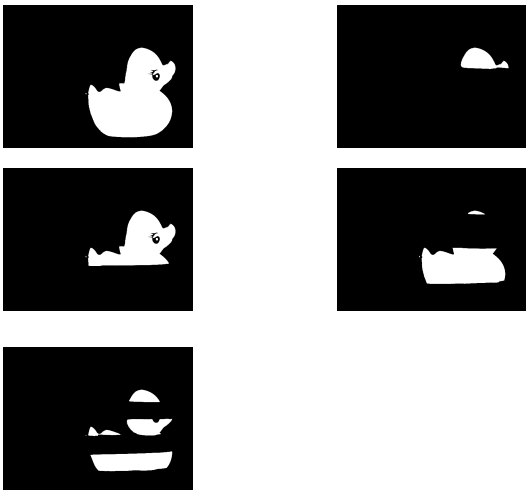

Fig. 10 Captured images with the projections of horizontal Gray-coded patterns.

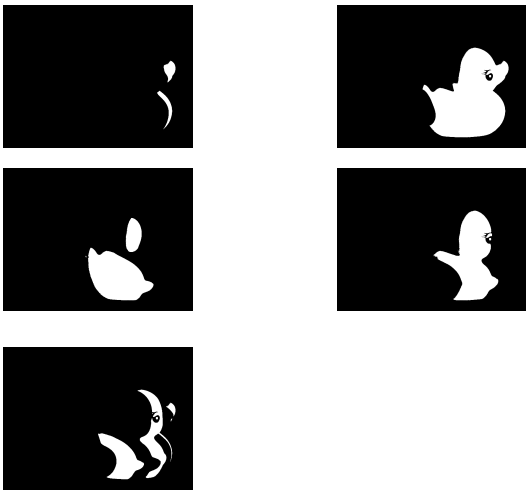

Fig. 11 Captured images with the projections of vertical Gray-coded patterns.

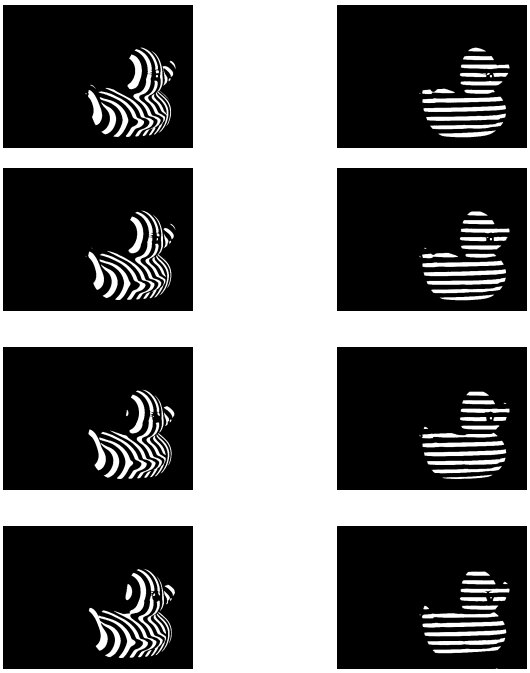

Fig. 12 Captured images with the projections of phase-shifting Gray-coded patterns

Fig. 13 Ground truth

6.2 Underwater 3D shape reconstruction

6.2.1 Correspondence Search with Regular Structured Light Patterns

In this part, we would like to realize 3D shape reconstruction of underwater object by projecting regular structured light patterns on the object in order to obtain the ground truth 3D shape.

Here we assume the projector has 256×256 resolution and we projected 5-bits Gray-coded pattern and 2-bits phase-shifting Gray- coded patterns on the object. That is, we took 9 images in total (Figs. 10, 11, and 12). Once we obtain the one-to-one correspondence between camera and projector by decoding these regular structured light patterns, we then can realize an underwater 3D shape reconstruction by using the method described in Section 5 as the ground truth (Fig. 13).

6.2.2 Correspondence Search with Single Grid Pattern

In this part, we would like to realize one-shot underwater 3D shape reconstruction.

We first projected a single grid pattern onto the surface of an underwater object and captured it by a camera (Fig. 14). Such grid pattern is periodically color-coded (8 lines in a cycle) which indicates that it cannot provide absolute corresponding projector pixel locations. From the captured image, the continuous regions were detected in both horizontal (y-axis) and vertical (x-axis) directions as shown in Fig. 15. The relative correspondences of projector were provided after unwrapping the values in each region respectively (Fig. 16).

Once all of the relative one-to-one correspondence between projector and camera were computed, the absolute correspondences of projector could be estimated by employing the co-planarity constraint in water. Finally, the 3D shape reconstruction was done by using the method described in Section 5 (Fig. 17). The computational time of this part took less than 10 seconds on an Intel Core-i7 2.3GHz PC.

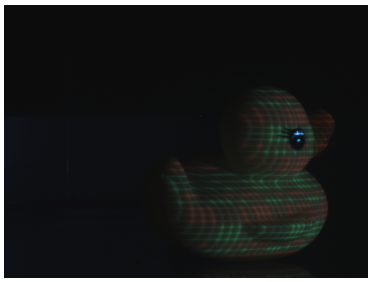

Fig. 14 Captured image with static grid pattern

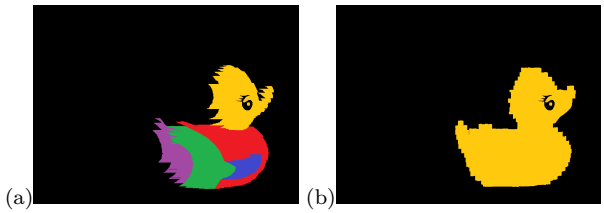

Fig. 15 Continuous regions detection (a) vertical (x-axis) direction, (b) horizontal (y-axis) direction.

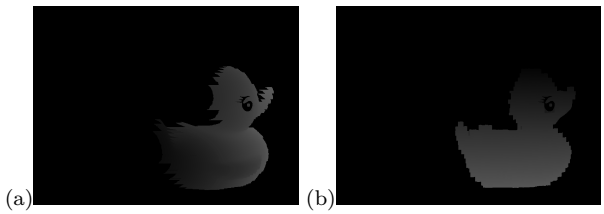

Fig. 16 Relative correspondences of projector (a) vertical (x-axis) direction, (b) horizontal (y-axis) direction.

Fig. 17 3D shape reconstruction result using single grid pattern

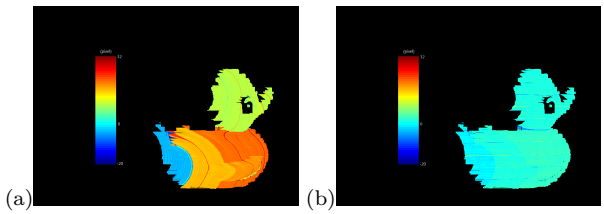

Fig. 18 Region-wise error distribution of unknown shifts (a) vertical (x-axis) direction, (b) horizontal (y-axis) direction.

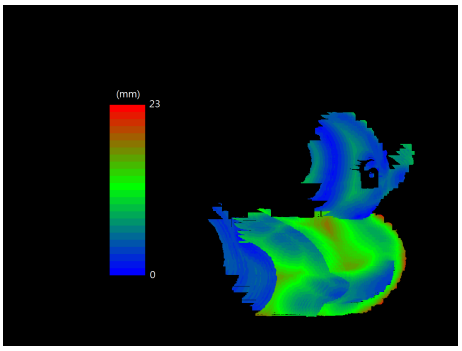

Fig. 19 Error distribution of one-shot 3D shape reconstruction.

6.2.3 Error Distribution

In our situation, if there are two pixels on the projector image plane that are apart from each other by only one pixel, then the two corresponding 3D points in water estimated by the method described in Section 5 differ around 1.3 millimeters from each other.

In one-shot underwater 3D shape reconstruction, the region-wise error distributions of unknown shifts for both vertical (x-axis) direction and horizontal (y-axis) direction can be shown in Fig. 18, which were obtained by calculating the differences between the estimated unknown shifts and the unknown shifts computed by utilizing the information of ground truth. The error of unknown shift in projector image ranged from -20 pixels to 32 pixels in vertical (x-axis) direction and ranged from -10 pixels to 10 pixels in horizontal (y-axis) direction, which implied that the deviation of the outcome of 3D shape reconstruction would be around 41.6 millimeters at most.

In order to evaluate the accuracy of such one-shot reconstruction result by the proposed method with a single grid pattern, we calculated the error distances from the 3D points of ground truth in water in millimeters. The 3D points of the ground truth were chosen based on the nearest neighbor search. Fig. 19 illustrates the error distribution of the one-shot reconstruction.

As shown in Fig. 18 and Fig. 19, the region-wise errors of unknown shifts caused the error distribution of the reconstruction result region-wise. Though the calibration / line detection errors might be the source of the offset estimation failure, this region-wise approach is promising due to the fact that it can be robust to noise by integrating many pixel-wise observations in the same region. Nevertheless, once the noise / error accumulates too much, the offset estimation might fail for the entire region.

7. Conclusion

In this paper, we proposed a novel one-shot 3D shape reconstruction algorithm using a projector-to-camera pair for objects in water. We mainly dealt with the refraction encountered in underwater environment. We resolved the ambiguity that occurs in the one-shot based correspondence search by employing the refractive underwater geometry. More precisely, the one-to-one correspondence between projector and camera pixel locations can be established by employing the co-

planarity constraint between 3D rays in water emitted from the camera and the projector through an observed image with the projected one-shot pattern in underwater environment.

We have employed a virtual camera model to overcome the refractive distortions geometrically and have successfully realized a one-shot 3D shape reconstruction in underwater environment in practice.

However, there are still rooms for improvement and are worthy for future study. For example, the accuracy of the current result of one-shot underwater 3D shape reconstruction can possibly be improved by adding some constraints related to the continuity of the surface of the object during the process of reconstruction. Moreover, the computational time toward real-time underwater 3D scanning can be improved.

References

[1] Amit Agrawal, Srikumar Ramalingam, Yuichi Taguchi, and Visesh Chari. A theory of multi-layer flat refractive geometry. pages 3346–3353, 2012.

[2] Anne Jordt-Sedlazeck, Daniel Jung, and Reinhard Koch. Refractive plane sweep for underwater images. In *Pattern Recognition - 35th German Conference, GCPR 2013, Saarbrücken, Germany, September 3-6, 2013. Proceedings*, pages 333–342, 2013.

[3] Lai Kang, Lingda Wu, and Yee-Hong Yang. Two-view underwater structure and motion for cameras under flat refractive interfaces. In *Computer Vision - ECCV 2012 - 12th European Conference on Computer Vision, Florence, Italy, October 7-13, 2012, Proceedings, Part IV*, pages 303–316, 2012.

[4] Ryo Kawahara, Shohei Nobuhara, and Takashi Matsuyama. A pixel-wise varifocal camera model for efficient forward projection and linear extrinsic calibration of underwater cameras with flat housings. In *The IEEE International Conference on Computer Vision (ICCV) Workshops*, June 2013.

[5] J. M. Lavest, G. Rives, and J. T. Lapresté. *Underwater Camera Calibration*, pages 654–668. Springer Berlin Heidelberg, Berlin, Heidelberg, 2000.

[6] Hiroki Morinaga, Hirohisa Baba, Marco Visentini Scarzanella, Hiroshi Kawasaki, Ryo Furukawa, and Ryusuke Sagawa. Underwater active oneshot scan with static wave pattern and bundle adjustment. In Thomas Bräunl, Brendan McCane, Mariano Rivera, and Xinguo Yu, editors, *PSIVT*, volume 9431 of *Lecture Notes in Computer Science*, pages 404–418. Springer, 2015.

[7] Ryusuke Sagawa, Hiroshi Kawasaki, Shota Kiyota, and Ryo Furukawa. Dense one-shot 3d reconstruction by detecting continuous regions with parallel line projection. In Dimitris N. Metaxas, Long Quan, Alberto Sanfeliu, and Luc J. Van Gool, editors, *ICCV*, pages 1911–1918. IEEE Computer Society, 2011.

[8] Ryusuke Sagawa, Yuichi Ota, Yasushi Yagi, Ryo Furukawa, and Naoki Asada. Dense 3d reconstruction method using a single pattern for fast moving object. In *in Proc. of 2009 IEEE 12th ICCV*, pages 1779–1786, 2009.

[9] Ryusuke Sagawa, Kazuhiro Sakashita, Nozomu Kasuya, Hiroshi Kawasaki, Ryo Furukawa, and Yasushi Yagi. Grid-based active stereo with single-colored wave pattern for dense one-shot 3d scan. *2011 International Conference on 3D Imaging, Modeling, Processing, Visualization and Transmission*, 00:363–370, 2012.

[10] Anne Sedlazeck and Reinhard Koch. Calibration of housing parameters for underwater stereo-camera rigs. In *British Machine Vision Conference, BMVC 2011, Dundee, UK, August 29 - September 2, 2011. Proceedings*, pages 1–11, 2011.